Narrow superconducting window in $LaFe_{1-x}Ni_xAsO$

Guanghan Cao,[1,*] Shuai Jiang,[1] Xiao Lin,[1] Cao Wang,[1] Yuke Li,[1] Zhi Ren,[1] Qian Tao,[1] Chunmu Feng,[2] Jianhui Dai,[1] Zhu'an Xu,[1,†] and Fu-Chun Zhang[1,3]

[1]*Department of Physics, Zhejiang University, Hangzhou 310027, China*

[2]*Test and Analysis Center, Zhejiang University, Hangzhou 310027, China*

[3]*Department of Physics, The University of Hong Kong, Hong Kong, China*

(Received 8 December 2008; revised manuscript received 31 March 2009; published 5 May 2009)

We have studied Ni-substitution effect in $LaFe_{1-x}Ni_xAsO$ ($0 \le x \le 0.1$) by the measurements of x-ray diffraction, electrical resistivity, magnetic susceptibility, and heat capacity. The nickel doping drastically suppresses the resistivity anomaly associated with spin-density-wave ordering in the parent compound. Superconductivity emerges in a narrow region of $0.03 \le x \le 0.06$ with the maximum T_c of 6.5 K at $x=0.04$, where enhanced magnetic susceptibility shows up. The upper critical field at zero temperature is estimated to exceed the Pauli paramagnetic limit. The much lowered T_c in comparison with $LaFeAsO_{1-x}F_x$ system is discussed.

DOI: 10.1103/PhysRevB.79.174505 PACS number(s): 74.70.Dd, 72.15.Qm, 74.62.Dh

I. INTRODUCTION

The discovery of superconductivity at 26 K in $LaFeAsO_{1-x}F_x$ (Ref. 1) and the subsequent findings of the enhanced superconductivity with T_c up to 56 K (Refs. 2–5) in a series of iron-arsenides have stimulated enormous research interest. It has been suggested that both electronic correlations and multiorbital/band effects should play important roles.[6–12] The prototype parent compound, LaFeAsO, undergoes a structural phase transition at 155 K,[13,14] followed by a collinear antiferromagnetic (AFM) spin-density-wave (SDW) transition at lower temperature.[13,15] Electron/hole doping into the FeAs layers suppresses the long-range SDW order, in favor of superconductivity.[15,16] This phenomenon is apparently analogous to that in cuprates, where superconductivity is induced by doping of charge carriers into an AFM Mott insulator. The iron arsenides, however, also show remarkable differences from the cuprates. For example, the parent compounds of iron arsenides show itinerant character of Fe $3d$ electrons,[17–20] while Cu $3d$ electrons in the parent compounds of the cuprates are localized.

As inferred in the band structure calculations for LaOMAs As (M= Mn, Fe, Co and Ni),[21] *Fe-site doping* with Co or Ni in the parent compounds of iron arsenides may also introduce additional electrons, hence possibly inducing superconductivity. This has been experimentally realized for the Co doping with $T_c \sim 13$ K in $LaFe_{1-x}Co_xAsO$ (Refs. 22 and 23) and $T_c=22$ K in $BaFe_{1.8}Co_{0.2}As_2$.[24] Since Ni atoms have one more electron than Co, one would expect that substitution of Fe with Ni introduces carriers more effectively. A possible hint comes from the Ni-based arsenide analog, LaNiAsO, which is a superconductor with $T_c \sim 2.5$ K.[25,26] The normal state of the LaNiAsO superconductor is Pauli paramagnetic,[26] suggesting that the Ni $3d$ electrons have an itinerant character.

In this paper we report the realization of superconductivity in $LaFe_{1-x}Ni_xAsO$($0 \le x \le 0.1$). Superconductivity has been observed in a narrow region of $0.03 \le x \le 0.06$ with a lowered maximum T_c of 6.5 K. The optimal doping level is found to be about half of that in $LaFe_{1-x}Co_xAsO$ (Ref. 23) system. The occurrence of superconductivity by Ni doping at Fe site contrasts sharply with severe suppression of superconductivity by the Cu-site doping with Ni in cuprate superconductors.

II. EXPERIMENTAL

Polycrystalline $LaFe_{1-x}Ni_xAsO$ samples were synthesized by solid state reaction in vacuum, similar to previous report.[23] Powders of LaAs, La_2O_3, FeAs, Fe_2As and NiO were weighed according to the stoichiometric ratios of $LaFe_{1-x}Ni_xAsO$ (x=0, 0.01, 0.02, 0.03, 0.04, 0.05, 0.06, 0.08, and 0.1), and thoroughly mixed in an agate mortar and pressed into pellets under a pressure of 2000 kg/cm^2. The pellets were sealed in evacuated quartz tubes, then heated uniformly at 1433 K for 48 h, and finally cooled by shutting off the furnace.

The resultant samples were characterized by powder x-ray diffraction (XRD) with Cu $K\alpha$ radiation. The XRD diffractometer system was calibrated using standard Si powders. The detailed structural parameters were obtained by Rietveld refinements, using the step-scan XRD data with $10° \le 2\theta \le 120°$. The typical R values of the refinements are: $R_F \sim 2.8\%$, $R_I \sim 4.6\%$, and $R_{wp} \sim 13\%$. The goodness-of-fit parameter, $S=R_{wp}/R_{exp} \sim 1.6$, indicating good reliability of the refinement.

The electrical resistivity was measured with a standard four-terminal method. Samples were cut into a thin bar with typical size of $4 \times 2 \times 0.5$ mm^3. Gold wires were attached onto the samples' abraded surface with silver paint. The size of the contact pads leads to a total uncertainty in the absolute values of resistivity of 10%. The measurements of magnetoresistance and heat capacity were carried out on a Quantum Design physical property measurement system (PPMS-9). Temperature dependence of magnetization was measured on a Quantum Design magnetic property measurement system (MPMS). In the measurements of normal-state susceptibility, the background data from the sample holder were removed. For the measurement of the superconducting (SC) transitions, both the zero-field cooling (ZFC) and field cooling (FC) protocols were employed under the field of 10 Oe.

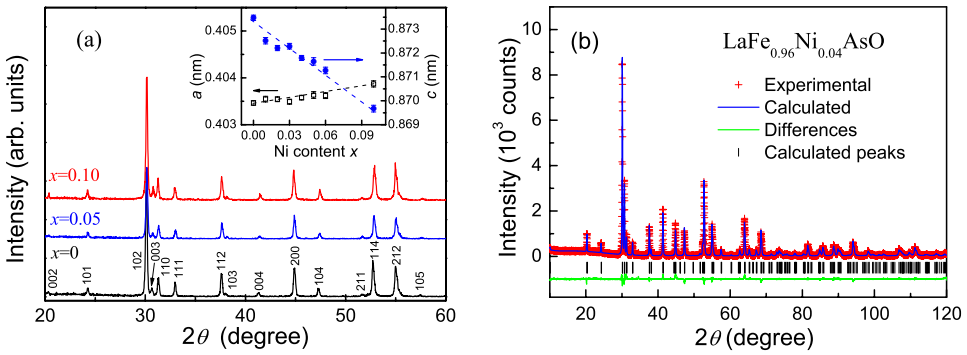

FIG. 1. (Color online) (a) Powder x-ray diffraction patterns of representative samples of $LaFe_{1-x}Ni_xAsO$. The inset shows the lattice constants as functions of Ni content. (b) An example of Rietveld refinement profile for $x=0.04$.

III. RESULTS AND DISCUSSION

Figure 1(a) shows XRD patterns of the representative samples of $LaFe_{1-x}Ni_xAsO$. The XRD peaks are well indexed based on a tetragonal cell with the space group of $P4/nmm$, indicating that the samples are essentially single phase. The lattice parameters are plotted in the inset as functions of x. With the increase in Ni doping the a axis increases slightly, while the c axis shrinks remarkably. The cell volume is consequently decreased by the incorporation of Ni.

The crystallographic parameters were obtained by the Rietveld refinement [Fig. 1(b)] based on ZrCuSiAs-type structure. Table I compares the structural data of undoped and Ni-doped (by 4 at. %) samples. The Ni doping enlarges the Fe-Fe spacing slightly, but compresses the FeAs layers significantly. In other word, the most remarkable effect of Ni doping on the crystal structure is that As atoms are pulled toward the Fe planes.

Figure 2 shows temperature dependence of resistivity (ρ) in $LaFe_{1-x}Ni_xAsO$. The parent compound shows a resistivity anomaly below 155 K. This resistivity anomaly has been identified as due to a structural phase transition associated with SDW instability.[13–15,27] Upon doping with 1% and 2% Ni, the anomaly temperature T_{anom} is suppressed to 105 and 75 K, respectively. As x increases to 0.03, a tiny anomaly in ρ can be detectable at 50 K, meanwhile the resistivity drops to zero below 5.5 K, suggesting emergence of superconductivity. The SC transition temperatures are 6.5 and 3.4 K for the samples of $x=0.04$ and 0.05, respectively, as shown in the inset of Fig. 2.

TABLE I. Crystallographic data of $LaFe_{1-x}Ni_xAsO$ ($x=0$ and 0.04) at room temperature. The space group is $P4/nmm$. The atomic coordinates are as follows: La (0.25,0.25,z); Fe/Ni (0.75,0.25,0.5); As (0.25,0.25,z); O (0.75,0.25,0).

Compounds	LaFeAsO	$LaFe_{0.96}Ni_{0.04}AsO$
a (Å)	4.0357(3)	4.0376(3)
c (Å)	8.7378(6)	8.7208(6)
V (Å^3)	142.31(2)	142.17(2)
z of La	0.1411(2)	0.1422(2)
z of As	0.6513(3)	0.6505(3)
FeAs-layer thickness (Å)	2.644(2)	2.624(2)
Fe-Fe spacing (Å)	2.8536(3)	2.8550(3)
As-Fe-As angle (°)	113.5(1)	114.0(1)

Figure 3 shows SC diamagnetic transitions in $LaFe_{1-x}Ni_xAsO$. Although samples with $x \leq 0.02$ show no diamagnetic signal above 1.8 K, magnetic expelling/screening can be clearly seen for $0.03 \leq x \leq 0.06$ at low temperatures. The magnetic shielding fraction of the sample of $x=0.04$ is estimated to be 45%, confirming bulk superconductivity. The diamagnetic curve shows steplike feature, probably due to sample inhomogeneity and/or an intergrain SC transition. The diamagnetic signal for other SC samples is much lower, implying that the SC region would be even narrower if samples were homogeneous. Similar phenomena were also observed in $LaFe_{1-x}Co_xAsO$ systems.[22,23]

To verify bulk superconductivity further, we performed specific-heat (C) measurement for the sample of $x=0.04$. The result is shown in Fig. 4. A specific-heat anomaly can be seen at $T_c \sim 6.5$ K (a tiny anomaly at about 8 K might be related to the trace residual SDW transition). In the temperature range from 6.7 to 10 K, the specific heat can be well described by the sum of electronic and lattice contributions: $C=\gamma T+\beta T^3$. Therefore, the linear fit for C/T versus T^2 gives the electronic specific-heat coefficient $\gamma = 5.74$ mJ/(mol K^2) and the lattice specific-heat coefficient $\beta=0.254$ mJ/(mol K^4). The Debye temperature θ_D is then calculated to be 285 K, using the formula $\theta_D=(12\pi RN/5\beta)^{1/3}$, where $N=4$ and $R=8.314$ J/(mol K). The value of θ_D is close to that of LaFeAsO (282 K, Ref. 15) and that of $LaFeAsO_{0.89}F_{0.11}$ (308 K, Ref. 28). The value of γ is also comparable to those of $LaFeAsO_{1-x}F_x$ samples (Refs. 15 and 28).

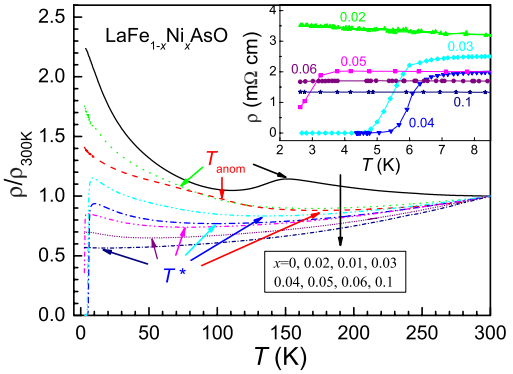

FIG. 2. (Color online) Temperature dependence of resistivity of $LaFe_{1-x}Ni_xAsO$ samples. The data are normalized to $\rho_{300\ K}$. The temperatures of resistivity peaks/humps (T_{anom}) and minima (T^*) are, respectively, marked. The inset shows an expanded plot.

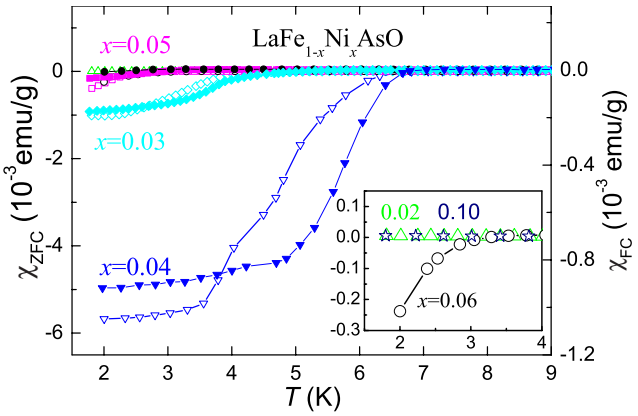

FIG. 3. (Color online) Temperature dependence of magnetic susceptibility in $LaFe_{1-x}Ni_xAsO$. Note that the open and filled symbols denote ZFC and FC data, respectively. The inset is an expanded plot for showing the data of $x=0.02$, 0.06 and 0.10.

After subtracting the lattice contribution to the specific heat, the specific-heat jump at the SC transition can be obviously seen, confirming bulk superconductivity. The dimensionless parameter $\Delta C_e/\gamma T$ at T_c is estimated to be 0.73, much lower than the expected value of 1.43 for an isotropic SC gap. This observation is similar to that in $LaFeAsO_{1-x}F_x$.[28] One may also see two transitions at 5 and 6.5 K, in accordance with the above steplike diamagnetic susceptibility curve. This phenomenon is probably due to the sample inhomogeneity and/or intergrain SC transition as mentioned above, however, the possibility of multiband superconductivity cannot be fully ruled out.

Figure 5 shows suppression of SC transition in resistivity under magnetic fields for the sample of $x=0.04$. The applied field shifts the SC transition toward lower temperatures, and the transition becomes broadened. The inset plots the temperature dependence of T_c (H), defined as the temperature where the resistivity falls to one-half of the normal-state value. The initial slope $\mu_0 \partial H_{c2}/\partial T$ near T_c is -3.81 T/K, which leads to an estimated upper critical field at zero-field $\mu_0 H_{c2}(0) \sim 17$ T using Werthamer-Helfand-Hohenberg model (Ref. 29). This value of upper critical field exceeds the

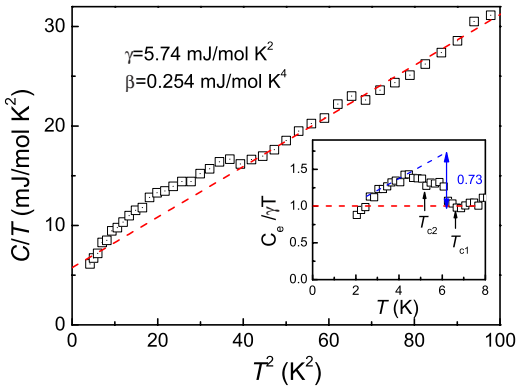

FIG. 4. (Color online) Curve of C/T versus T^2 for the sample of $x=0.04$ in $LaFe_{1-x}Ni_xAsO$ system under zero field. The inset shows $C_e/\gamma T$ as a function of temperature, where C_e denotes electronic specific heat.

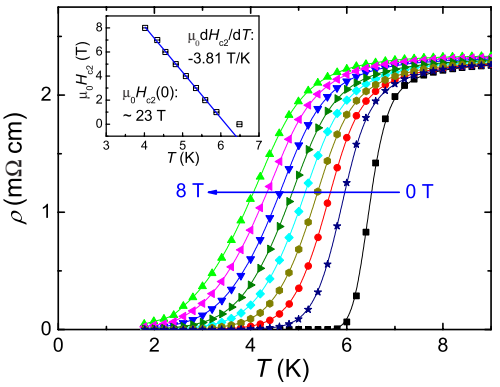

FIG. 5. (Color online) SC transitions in resistivity under magnetic fields ($\mu_0 H=0$, 1, 2, 3, 4, 5, 6, 7, and 8 T) for $LaFe_{0.96}Ni_{0.04}AsO$ sample. The inset shows the upper critical fields as a function of temperature.

Pauli paramagnetic limit $\mu_0 H_P = 1.84 T_c \sim 12$ T (Ref. 30). Similar observations have been reported in $LaFeAsO_{1-x}F_x$ system.[31,32] The high critical field makes $LaFe_{0.96}Ni_{0.04}AsO$ fundamentally different from the LaFeNiO superconductor (Refs. 25 and 26).

The normal-state susceptibility χ of the Ni-doped samples is shown in Fig. 6. The $\chi(T)$ are characterized by linear decrease at high temperatures as well as Curie-like upturn below ~ 100 K. The Curie-like upturn was found to be sensitive to sample's quality. Generally, better sample shows smaller susceptibility upturn. Thus, the susceptibility upturn is mainly due to an extrinsic origin (such as defects and trace impurities). The linear T-dependence of χ was experimentally demonstrated in $LaFeAsO_{1-x}F_x$ (Ref. 33) and $BaFe_2As_2$ (Ref. 34) systems, and was discussed in terms of the "preformed SDW moments".[35] The measured $\chi(T)$ can thus be fitted with the formula,

$$\chi(T) = \chi_0 + \alpha T + \frac{C}{T}, \tag{1}$$

where the T-independent term χ_0 contains Pauli paramagnetic susceptibility (χ_P) (Ref. 36) from itinerant electrons

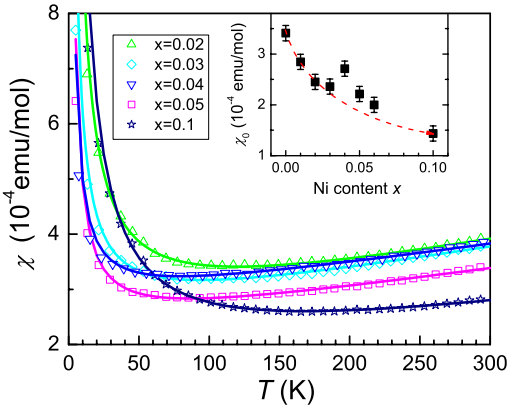

FIG. 6. (Color online) Temperature dependence of magnetic susceptibility in $LaFe_{1-x}Ni_xAsO$. The applied field is 1000 Oe. The solid lines are fitted result using Eq. (1). The inset plots the T-independent term χ_0 as a function of Ni content. The dashed line is a guide to the eyes.

TABLE II. Fitted parameters using Eq. (1) for $LaFe_{1-x}Ni_xAsO$ system. The units of χ_0, α, and C are emu mol^{-1}, emu mol^{-1} K^{-1}, and emu K mol^{-1}, respectively.

Samples	$\chi_0(\times 10^4)$	$\alpha(\times 10^7)$	C
$x=0$	3.27	3.6	0.0045
$x=0.01$	2.85	3.0	0.0070
$x=0.02$	2.45	4.1	0.0056
$x=0.03$	2.36	4.3	0.0038
$x=0.04$	2.71	3.4	0.0021
$x=0.05$	2.22	3.6	0.0027
$x=0.06$	2.00	3.8	0.0035
$x=0.10$	1.44	3.5	0.0098

and Larmor diamagnetic susceptibility (χ_{core}) from ionic cores. It is noted that the change in χ_0 with the Ni doping is primarily due to the variation of χ_P.

To avoid the influence of the structural transition for $0 \le x \le 0.02$, we made the fitting using different range of data as follows: 160 K $\le T \le$ 300 K for $x=0$, 110 K $\le T \le$ 300 K for $x=0.01$, 75 K $\le T \le$ 300 K for $x=0.02$, 50 K $\le T \le$ 300 K for $x=0.03$, and 30 K $\le T \le$ 300 K for $x>0.03$. The fitted parameters are listed in Table II. It is shown that the α values are about 4×10^{-7} emu mol^{-1} K^{-1}, almost independent of Ni-doping x, similar to the case reported in $LaFeAsO_{1-x}F_x$.[33] The extracted χ_0, shown in the inset of Fig. 6, tends to decrease with increasing Ni-doping, with an enhancement in the SC regions centered at $x=0.04$. The decrease in χ_0 with x reflects the electron doping since band calculations show a negative $dN(E)/dE$ at Fermi level.[17,21] The extra susceptibility in the SC regime resembles the behavior of thermopower in $SmFe_{1-x}Co_xAsO$ system,[23] implying the importance of spin fluctuations for the superconductivity. Besides, the enhanced spin fluctuations are also evidenced by the relatively high value of Wilson ratio, defined as $R_W=\frac{\pi^2 k_B^2 \chi_P}{3\gamma\mu_B^2}$. Since the χ_{core} of $LaFe_{1-x}Ni_xAsO$ is about -1.0×10^{-4} emu mol^{-1},[37] χ_P is thus about 3.7×10^{-4} emu mol^{-1} for $x=0.04$, giving R_W of 4.7.

It is noted that the maximum T_c (6.5 K) in $LaFe_{1-x}Ni_xAsO$ is merely one fourth of that in $LaFeAsO_{1-x}F_x$,[1] and half of that in $LaFe_{1-x}Co_xAsO$.[23] The lowered T_c in the Co-doped system was discussed in terms of the relatively small As-Fe-As angle,[23] according to an empirical structural rule for T_c variations.[38] However, the As-Fe-As angle of $LaFe_{0.96}Ni_{0.04}AsO$ is almost the same as that of $LaFe_{0.925}Co_{0.075}AsO$. Therefore, the much lowered T_c in $LaFe_{1-x}Ni_xAsO$ system should be caused by the reason other than structural aspect.

Let us turn to examine the normal-state property to find the possible clues. The normal-state resistivity strikingly exhibits a semiconductinglike behavior above T_c, as shown in Fig. 2. At first glance, the resistivity upturn at low temperatures might be ascribed to Anderson localization owing to the Ni incorporation, which might account for the lowered T_c. This scenario of disorder-induced localization would lead to a more profound resistivity upturn or higher T^* (resistivity minimum temperature) with the increase in Ni doping. However, the $\rho(T)$ curves in Fig. 2 show that T^* *decreases* monotonically with increasing x. Therefore, the evolution of the resistivity upturn with Ni doping suggests that Anderson localization is unlikely to be the main reason for the lowered T_c.

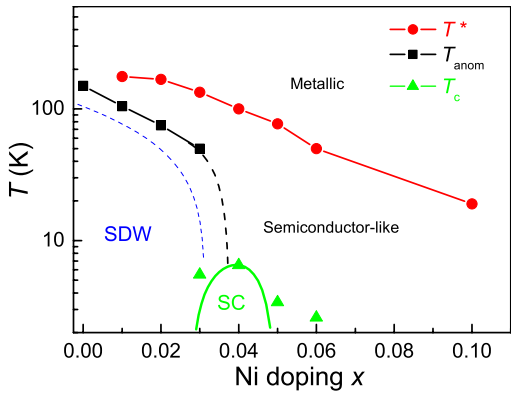

FIG. 7. (Color online) Electronic phase diagram for $LaFe_{1-x}Ni_xAsO$, showing a narrow SC window. The short dashed line schematically shows the SDW transition temperature, which is tens of Kelvin below T_{anom} (Ref. 13). Note that the vertical axis is in logarithmic scale.

In the framework of a coherent-incoherent scenario,[39] the itinerant carriers and the local magnetic moments coexist in the undoped iron arsenides. Based on the logarithmic upturn of resistivity, a spin-flip scattering between the itinerant charge carriers and the local moments in the undoped FeAs layers has very recently been proposed.[40] It is noted that the spin-flip scattering (actually analog to Kondo effect) is already there in the parent compound. Upon electron doping, T^* is suppressed due to the decrease in $N(E_F)$, as the Kondo energy scale $T_K \propto \sqrt{JN(E_F)}\exp[-1/JN(E_F)]$ with J being the Kondo coupling constant. In the case of Ni doping, both extra itinerant $3d$ electrons and *stabilized* local moments (as inferred from the band structure calculation[21]) are introduced. For the same electron doping level, one would expect an enhanced spin-flip scattering in the Ni-doped system. The spin-flip scattering competes with the SC Cooper pairing, which explains the suppression of T_c. Therefore, the narrow SC region as well as the much lowered T_c in $LaFe_{1-x}Ni_xAsO$ system is here ascribed to be a combined effect from the competing Kondo-like interactions, Anderson localization, as well as the structural variation.

Very recently, the effectiveness of Ni doping for SC has been also demonstrated in $BaFe_2As_2$ (Ref. 41) and CaFeAsF (Ref. 42) systems. The $T_{c,max}$ are 20.5 and 12 K, respectively. The variations in T_c are possibly due to the Kondo-like interactions (not significant in Ni-doped $BaFe_2As_2$) as well as the structural difference. The bond angle of As-Fe-As in CaFeAsF is significantly smaller than that of LaFeAsO.

Figure 7 summarizes a SC phase diagram for $LaFe_{1-x}Ni_xAsO$ system. With Ni-doping, the SDW order is suppressed, followed by the emergence of superconductivity. The SC region is particularly narrow and the T_c is remarkably low, as compared with those of $LaFeAsO_{1-x}F_x$ and

TABLE III. Comparison of SC phase diagrams in $LaFe_{1-x}Co_xAsO$ (Ref. 23) and $LaFe_{1-x}Ni_xAsO$ (present work). $T_{c,max}$ denotes the maximum T_c at optimal doping level x_{opt}.

System	$LaFe_{1-x}Co_xAsO$	$LaFe_{1-x}Ni_xAsO$
SDW region	$0 \le x < 0.025$	$0 \le x < 0.02$
SC region	$0.025 \le x \le 0.125$	$0.03 \le x \le 0.06$
$T_{c,max}$(K)	13	6.5
x_{opt}	~0.075	~0.04
Normal-state ρ	Semiconducting	Semiconducting

$LaFe_{1-x}Co_xAsO$ (see Table III). The normal state is divided by the line of T^* into metallic and semiconducting regions. The "optimal" doping occurs at $x_{opt}=0.04$, which is about half of the x_{opt} of $LaFe_{1-x}Co_xAsO$. This observation further demonstrates the itinerant character of Ni $3d$ electrons. Here we emphasize that the occurrence of superconductivity by Ni doping contrasts sharply with the cuprate superconductors, where the substitution of Cu with Ni in CuO_2 planes severely destroys the superconductivity.[43]

ACKNOWLEDGMENTS

We would like to thank Y. Liu, Q. Si, H.Q. Yuan, and G.M. Zhang for useful discussions. This work is supported by the NSF of China (Contracts No. 10674119 and No. 10634030), National Basic Research Program of China (Contract No. 2007CB925001) and the PCSIRT of the Ministry of Education of China (Contract No. IRT0754) and RGC in HKSAR.

*ghcao@zju.edu.cn
†zhuan@zju.edu.cn

[1] Y. Kamihara, T. Watanabe, M. Hirano, and H. Hosono, J. Am. Chem. Soc. **130**, 3296 (2008).
[2] X. H. Chen, T. Wu, G. Wu, R. H. Liu, H. Chen, and D. F. Fang, Nature (London) **453**, 761 (2008).
[3] G. F. Chen, Z. Li, D. Wu, G. Li, W. Z. Hu, J. Dong, P. Zheng, J. L. Luo, and N. L. Wang, Phys. Rev. Lett. **100**, 247002 (2008).
[4] Z. A. Ren, W. Lu, J. Yang, W. Yi, X. L. Shen, Z. C. Li, G. C. Che, X. L. Dong, L. L. Sun, F. Zhou, and Z. X. Zhao, Chin. Phys. Lett. **25**, 2215 (2008).
[5] C. Wang, L. J. Li, S. Chi, Z. W. Zhu, Z. Ren, Y. K. Li, Y. T. Wang, X. Lin, Y. K. Luo, S. Jiang, X. F. Xu, G. H. Cao, and Z. A. Xu, Europhys. Lett. **83**, 67006 (2008).
[6] I. I. Mazin, D. J. Singh, M. D. Johannes, and M. H. Du, Phys. Rev. Lett. **101**, 057003 (2008).
[7] L. Boeri, O. V. Dolgov, and A. A. Golubov, Phys. Rev. Lett. **101**, 026403 (2008).
[8] X. Dai, Z. Fang, Y. Zhou, and F. C. Zhang, Phys. Rev. Lett. **101**, 057008 (2008).
[9] S. Raghu, X. L. Qi, C. X. Liu, D. J. Scalapino, and S. C. Zhang, Phys. Rev. B **77**, 220503(R) (2008).
[10] P. A. Lee and X. G. Wen, Phys. Rev. B **78**, 144517 (2008).
[11] Q. Si and E. Abrahams, Phys. Rev. Lett. **101**, 076401 (2008).
[12] K. Kuroki, S. Onari, R. Arita, H. Usui, Y. Tanaka, H. Kontani, and H. Aoki, Phys. Rev. Lett. **101**, 087004 (2008).
[13] C. de la Cruz, Q. Huang, J. W. Lynn, J. Li, W. Ratcliff II, H. A. Mook, G. F. Chen, J. L. Luo, N. L. Wang, and P. Dai, Nature (London) **453**, 899 (2008).
[14] T. Nomura, S. W. Kim, Y. Kamihara, M. Hirano, P. V. Sushko, K. Kato, M. Takata, A. L. Shluger, and H. Hosono, Supercond. Sci. Technol. **21**, 125028 (2008).
[15] J. Dong, H. J. Zhang, G. Xu, Z. Li, G. Li, W. Z. Hu, D. Wu, G. F. Chen, X. Dai, J. L. Luo, Z. Fang, and N. L. Wang, Europhys. Lett. **83**, 27006 (2008).
[16] H. H. Wen, G. Mu, L. Fang, H. Yang, and X. Y. Zhu, Europhys. Lett. **82**, 17009 (2008).
[17] D. J. Singh and M. H. Du, Phys. Rev. Lett. **100**, 237003 (2008).
[18] F. J. Ma and Z. Y. Lu, Phys. Rev. B **78**, 033111 (2008).
[19] V. Cvetkovic and Z. Tesanovic, Europhys. Lett. **85**, 37002 (2009).
[20] J. Wu, P. Phillips, and A. H. Castro Neto, Phys. Rev. Lett. **101**, 126401 (2008).
[21] G. Xu, W. Ming, Y. Yao, X. Dai, S.-C. Zhang, and Z. Fang, Europhys. Lett. **82**, 67002 (2008).
[22] A. S. Sefat, A. Huq, M. A. McGuire, R. Y. Jin, B. C. Sales, D. Mandrus, L. M. D. Cranswick, P. W. Stephens, and K. H. Stone, Phys. Rev. B **78**, 104505 (2008).
[23] C. Wang, Y. K. Li, Z. W. Zhu, S. Jiang, X. Lin, Y. K. Luo, S. Chi, L. J. Li, Z. Ren, M. He, H. Chen, Y. T. Wang, Q. Tao, G. H. Cao, and Z. A. Xu, Phys. Rev. B **79**, 054521 (2009).
[24] A. S. Sefat, R. Jin, M. A. McGuire, B. C. Sales, D. J. Singh, and D. Mandrus, Phys. Rev. Lett. **101**, 117004 (2008).
[25] Z. Li, G. F. Chen, J. Dong, G. Li, W. Z. Hu, D. Wu, S. K. Su, P. Zheng, T. Xiang, N. L. Wang, and J. L. Luo, Phys. Rev. B **78**, 060504(R) (2008).
[26] T. Watanabe, H. Yanagi, Y. Kamihara, T. Kamiya, M. Hirano, and H. Hosono, J. Solid State Chem. **181**, 2117 (2008).
[27] M. A. McGuire, A. D. Christianson, A. S. Sefat, B. C. Sales, M. D. Lumsden, R. Jin, E. A. Payzant, D. Mandrus, Y. Luan, V. Keppens, V. Varadarajan, J. W. Brill, R. P. Hermann, M. T. Sougrati, F. Grandjean, and G. J. Long, Phys. Rev. B **78**, 094517 (2008).
[28] Y. Kohama, Y. Kamihara, M. Hirano, H. Kawaji, T. Atake, and H. Hosono, Phys. Rev. B **78**, 020512(R) (2008).
[29] N. R. Werthamer, E. Helfand, and P. C. Hohenberg, Phys. Rev. **147**, 295 (1966).
[30] A. M. Clogston, Phys. Rev. Lett. **9**, 266 (1962); B. S. Chandrasekhar, Appl. Phys. Lett. **1**, 7 (1962).
[31] F. Hunte, J. Jaroszynski, A. Gurevich, D. C. Larbalestier, R. Jin, A. S. Sefat, M. A. McGuire, B. C. Sales, D. K. Christen, and D. Mandrus, Nature (London) **453**, 903 (2008).
[32] G. Fuchs, S.-L. Drechsler, N. Kozlova, G. Behr, A. Köhler, J. Werner, K. Nenkov, R. Klingeler, J. Hamann-Borrero, C. Hess, A. Kondrat, M. Grobosch, A. Narduzzo, M. Knupfer, J. Freudenberger, B. Büchner, and L. Schultz, Phys. Rev. Lett. **101**, 237003 (2008).
[33] R. Klingeler, N. Leps, I. Hellmann, A. Popa, C. Hess, A. Kon-

drat, J. Hamannborrero, G. Behr, V. Kataev, and B. Buechner, arXiv:0808.0708 (unpublished).
[34] X. F. Wang, T. Wu, G. Wu, H. Chen, Y. L. Xie, J. J. Ying, Y. J. Yan, R. H. Liu, and X. H. Chen, Phys. Rev. Lett. **102**, 117005 (2009).
[35] G. M. Zhang, Y. H. Su, Z. Y. Lu, Z. Y. Weng, D. H. Lee, and T. Xiang, arXiv:0809.3874 (unpublished).
[36] Here we ignore the discussion of Landau diamagnetism, because Landau susceptibility is 1/3 of χ_P when $m \approx m^*$.
[37] G. A. Bain and J. F. Berry, J. Chem. Educ. **85**, 532 (2008).
[38] J. Zhao, Q. Huang, C. de la Cruz, S. L. Li, J. W. Lynn, Y. Chen, M. A. Green, G. F. Chen, G. Li, Z. Li, J. L. Luo, N. L. Wang, and Pengcheng Dai, Nature Mater. **7**, 953 (2008).
[39] J. H. Dai, Q. Si, J. X. Zhu, and E. Abrahams, Proc. Natl. Acad. Sci. U.S.A. **106**, 4118 (2009).
[40] J. H. Dai, G. H. Cao, H. H. Wen, and Z. A. Xu, arXiv:0901.2787 (unpublished).
[41] L. J. Li, Y. K. Luo, Q. B. Wang, H. Chen, Z. Ren, Q. Tao, Y. K. Li, X. Lin, M. He, Z. W. Zhu, G. H. Cao, and Z. A. Xu, New J. Phys. **11**, 025008 (2009).
[42] S. Matsuishi, Y. Inoue, T. Nomura, Y. Kamihara, M. Hirano, and H. Hosono, New J. Phys. **11**, 025012 (2009).
[43] J. M. Tarascon, L. H. Greene, P. Barboux, W. R. McKinnon, G. W. Hull, T. P. Orlando, K. A. Delin, S. Foner, and E. J. McNiff, Phys. Rev. B **36**, 8393 (1987).